Nationaal Lucht- en Ruimtevaartlaboratorium
National Aerospace Laboratory NLR

NLR TP 96591

Experiences in Aeroelastic Simulation Practices

B.J.G. Eussen, M.H.L. Hounjet and R.J. Zwaan

~

DOCUMENT CONTROL SHEET

	ORIGINATOR'S REF.		SECURITY CLASS.m
	NLR TP 96591 U		**unclassified**

ORIGINATOR
National Aerospace Laboratory NLR, Amsterdam, The Netherlands

TITLE
Experiences in aeroelastic simulation practices

PRESENTED AT
EUROMECH colloquium 349, Göttingen, Germany, September 16-18, 1996

AUTHORS	DATE	pp	ref
B.J.G. Eussen, M.H.L. Hounjet and R.J. Zwaan	**961509**	**37**	**9**

DESCRIPTORS

ABSTRACT
The NLR system for the transonic aeroelastic analysis of aircraft is presented with an up to date account of applicability. Experience with recent applications to complex configurations is reported. Common problems arising from daily use are described together with the feedback to alleviate them. Also a first indication of critical components in the process cycle and turn-around time for every part is given.

Summary

The NLR system for the transonic aeroelastic analysis of aircraft is presented with an up to date account of applicability. Experience with recent applications to complex configurations is reported. Common problems arising from daily use are described together with the feedback to alleviate them. Also a first indication of critical components in the process cycle and turn-around time for every part is given.

Contents

(37 pages in total)

1 Nomenclature

Abbrev.	Description
AF	approximate factorisation
AESIM	aeroelastic simulation method for aircraft
BLOWUP	grid generator
CAR	unsteady full body panel method for arbitrary configurations
FOLDIT	geometry pre-processor
ICEM-CFD	Integrated Computer-aided Engineering and Manufacturing Software Application for Design Drafting and Numerical Control
LMS	Leuven Measurement Systems
GUL	unsteady lifting surface method for arbitrary configurations
NASTRAN	NASA structural analysis FEM package
PK	solution method for aeroelastic eigenvalue problem

2 Introduction

Rather unusually this introduction starts with an explanatory note to the realization of this paper. At the end of last year we at NLR encouraged our colleagues of Fokker Aircraft to present a paper on their experience of applying more or less advanced aeroelastic calculation methods in their design practice.

One of the topics would be their experience of using the aeroelastic simulation method that is being developed at NLR and of which a pilot version was tried out in the Fokker aeroelastic department.

An abstract for the presentation was drafted. Just before the deadline for submitting abstracts Fokker lost the financial support of its mother company DASA and fell into existential problems. At NLR we decided to go through with the presentation and submitted an abstract in time with a slightly adjusted content, in the hope and with the optimistic expectation that Fokker would survive somehow. The outcome is known: Fokker had to stop its design activities and at about the same time the abstract was accepted.

At NLR we had to consider once again the presentation and decided to continue also this time. However, title and topics to discuss have drifted away somewhat from what we had in mind at the first time. We nevertheless believe that they are of current interest and worth to be raised at this conference. What turned the scale in our decision to go through was that the essentials in the originally anticipated presentation would remain the same: The presentation of the status of the computational aeroelastic simulation method being developed by NLR and the discussion of some application aspects as experienced on the floor.

Fortunately, the NIVR continues for some time its funding for the development, while at the same time the adjustment of the method to make it usable towards military applications is accelerated, the latter being funded by the Royal Dutch Airforce. These financial means enable us to project a version of an aeroelastic simulation method which can be used commercially both for transport type as well as for fighter type aircraft.

In this presentation the simulation method and its potentialities will be presented and discussed.

The application aspects concern mainly topics which intimately affect to the users' effort on the floor:

1. surface and field grid generation for ’real’ aircraft components
2. information transfer on the fluid/structure interface and
3. the simulation and its analysis.

in relation to distinct aeroelastic needs.

3 Aeroelastic Simulation System

At NLR much effort has been spent to create a complete AEroelastic SIMulation system with a modular character, to be used primarily for the flutter certification of transport-type aircraft in the transonic speed regime. Time-accurate simulation of fluid and airframe structure interaction is emphasized. The AEroelastic SIMulation system is referred to as AESIM, after the name of the core program.

The AEroelastic SIMulation system is built around the AESIM core and consists of six independent main program modules, see figure 1:

- **FOLDIT**: surface grid generation
- **BLOWUP**: grid generation
- **NASAES**: elastomechanical data manipulation
- **AESIM** core
- Output interfacing e.g. to NASTRAN or LMS
- Linear methods library.

The AESIM core program is divided into 5 individual modules and contains those subroutines which are CPU intensive and make it possible to run the core in stand alone mode:

- **Interpolation:** Interpolation of elastomechanical and aerodynamic data.
- **Aero solver:** Time-accurate solving of aerodynamic equations.
- **Motion:** Either description of motions or solving of elastomechanical equations.
- **Monitoring:** Visualization of simulated data.
- **Postprocessing:** Recollection and assimilation of facts and figures of past simulation(s).

The various elements of this environment will now be discussed in more detail.

3.1 Surface grid generation

Consistent with aeroelastic requirements and discussed in 4 only the sub-structures of aircraft which are slender and have surfaces with low curvature (wing, tail and fin) need to be modeled quite well in obtaining the aerodynamic force in normal direction. Consequently the quality and density of the surface grids can be relaxed in the other areas. While the aeroelastician is not expected to be an expert surface modeler who creates a surface grid from scratch, the assumption is made that an initial surface grid is available which can be tuned to his needs in routine applications by the geometry preprocessor.

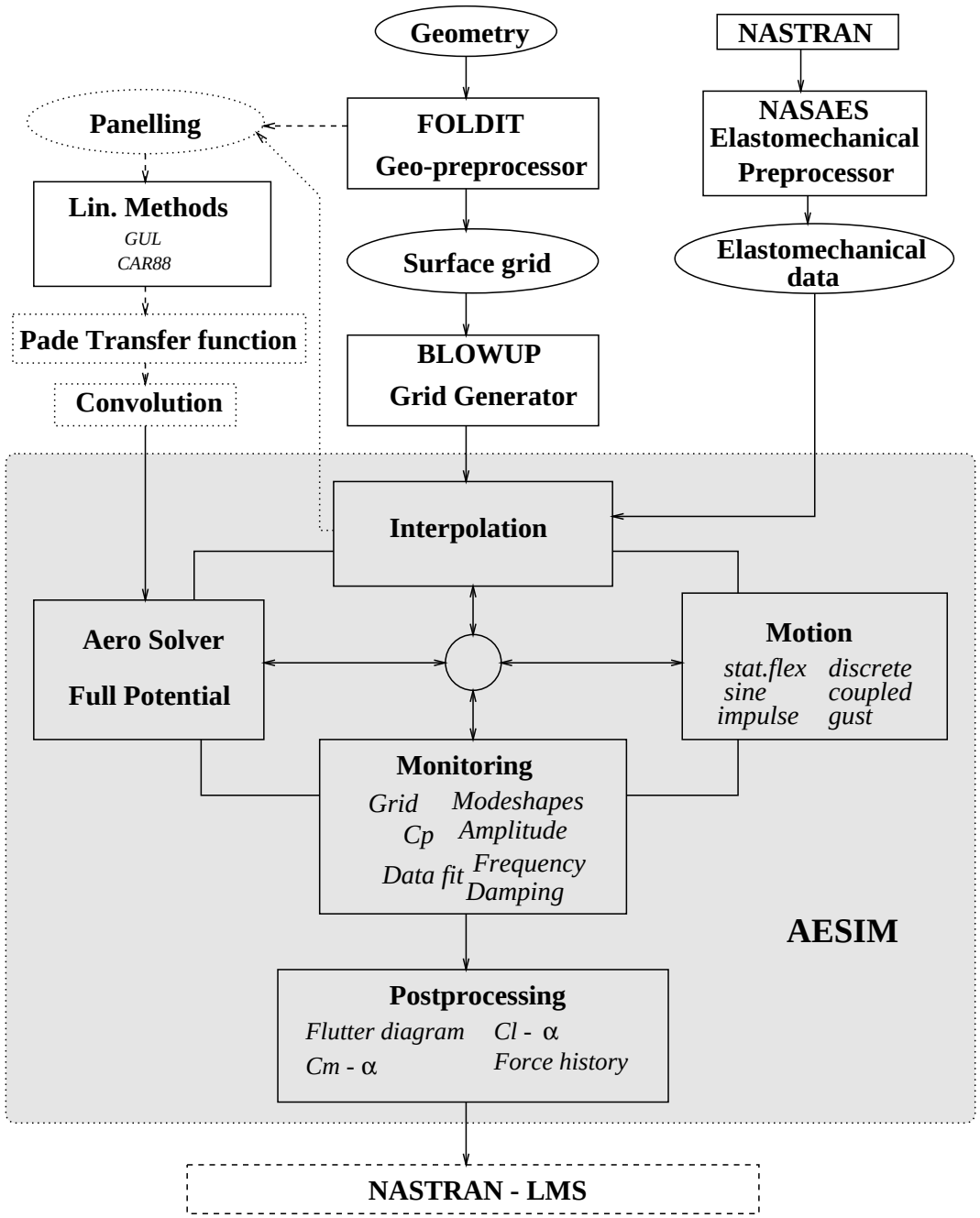

Fig. 1: AEroelastic SIMulation system

The geometry preprocessor FOLDIT generates a mono-block structured surface description and/or paneling of the complete aircraft with embedded upwind slits and downwind slits (wake surfaces) by assembling and interpolating separate parent surface grids (provided by the user by means of CAD/CAM programs). Instrumental in assisting the user in specifying the required spacing of each component in order to obtain smooth transitions is the so-called **domino** approach. This

approach requires the input of the spacings and the number of patches for a few of the parent surface grids which are interpolated (extrapolated) by the volume spline method 5 to the other surface grids. On the floor this means that the user only has to specify the leading and trailing edge resolution of the lifting parts.

FOLDIT also constructs the slits, allows for redistributions, data editing, data smoothing and stripping and tailors the configuration to aeroelastic needs. By this, considerable flexibility is offered to the aeroelastician who is not directed to other programs when minor changes have to be made for parametric studies. Also identification tags are generated which may be required by the interpolation of the elastomechanical data to the surface grid.

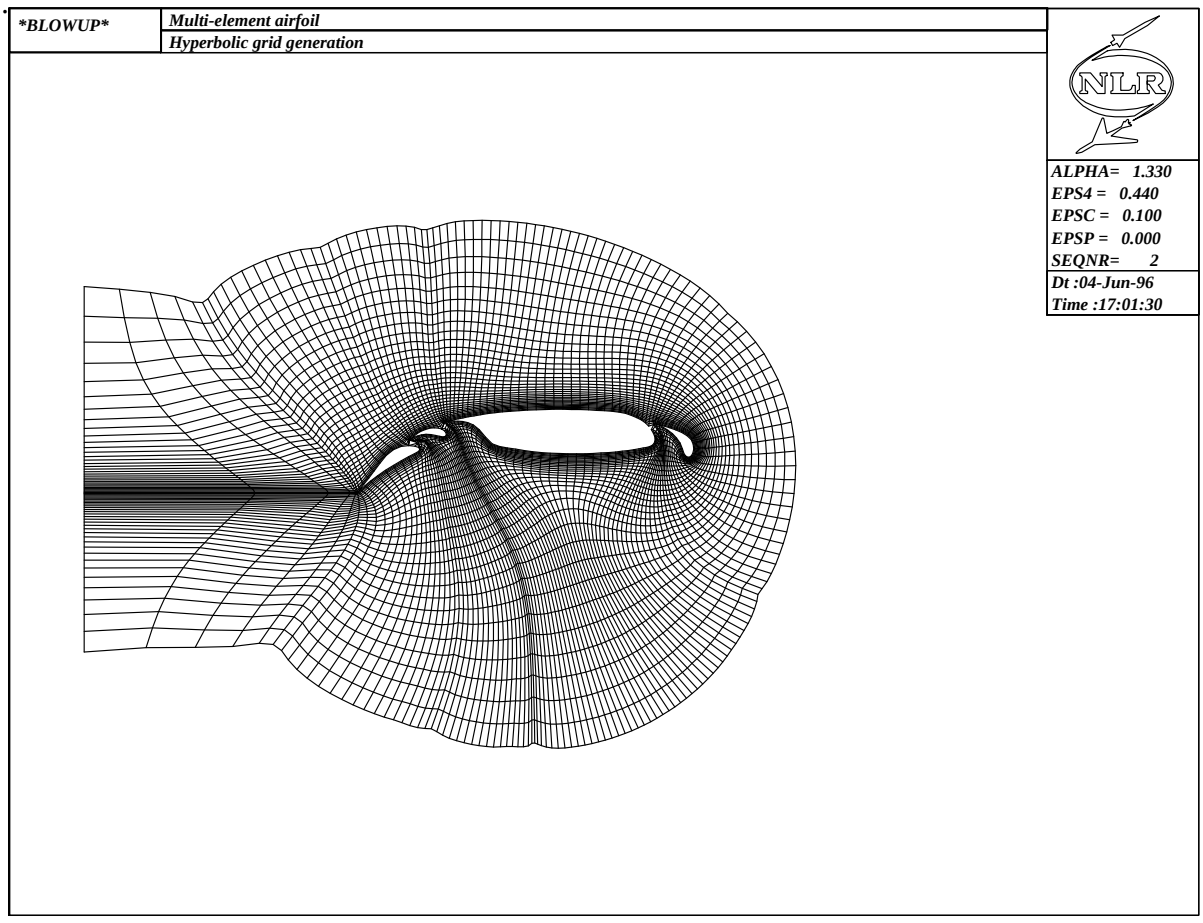

Fig. 2: Mono-block grid generated with a hyperbolic method about a multi-element airfoil

3.2 Grid generation

The grid generation is performed by the hyperbolic grid generation method BLOWUP described in 1. The effort to generate mono-block **HO** grids about the surface description of the complete aircraft with embedded upwind slits and downwind slits (wake surfaces) with mild concavities

is low enough to be applied by 'non-grid expert applicators'. The grids have acceptable quality about concave areas such as airfoil noses and wing-fuselage junctions. The consequence of some limitations in accuracy of the mono-block grid approach to more complex configurations is considered acceptable for aeroelastic applications rather than for performance design.

In the solution of the aforementioned modeling, additional in-plane dissipation terms are applied which are well described in 2. In addition, metric regularization terms have been developed to guarantee a proper behavior at axis, slit tips, strongly swept surfaces and non-smooth surface grids at wing-body junctions, tip regions, etc.

Also it has turned out that the constant implicitness parameters which are applied nowadays in most hyperbolic grid generators and control the out-of-plane dissipation required for preventing grid lines from crossing in the marching direction should be enhanced to prevent impairing the grid in convex zones. Therefore NLR has introduced a flexible implicitness parameter which can be applied more selective (small in convex zones and large in concave zones) and has worked well in all cases treated so far.

Many configurations can be gridded without angle control terms. In this case one relies on the dissipation terms for rendering concave domains. However, for some cases experiencing very strong concavities it might be necessary to use one of the following angle control options:

1. The terms are automatically derived from previously generated planes.
2. The terms are built from directions of the far field.
3. The terms are evaluated by a 2-D aerodynamic panel method.
4. The terms are provided by the surface(volume) spline method.
5. The terms are provided from a feedback procedure to prevent grid folding.

In addition BLOWUP has been equipped with the possibilities:

- Starting with an orthogonal grid.
- Post-elliptic smoothing with control functions to smooth the grid. The smoothing is primarily meant for smoothing the transition zone between the hyperbolic and the algebraic generated grid contours and in strong concave zones.
- Algebraic grid generation of grid surfaces in the far field (far front, far rear and far radial surfaces) can be applied when outer boundaries are to be prescribed.
- A hyperbolic shooting method is embedded to generate a grid with a fixed far field boundary distribution.
- Finally existing grids can be refined, enlarged and/or smoothed.

Also **CH,CO** topologies of the grid are provided for single wing applications of the AESIM code. Other topologies that are provided include **HH** ,**XH** and **OC**.

A complete description of the BLOWUP grid generator is presented in 8. We end this section by showing 2-D examples containing strong zones of concavities to demonstrate the viability of BLOWUP. The following 2-D grid C-type topology examples are presented: a multi-element airfoil in figure 2 and a cross-section of 2 fighter type fuselages mounted together at the tail and apex in figure 3.

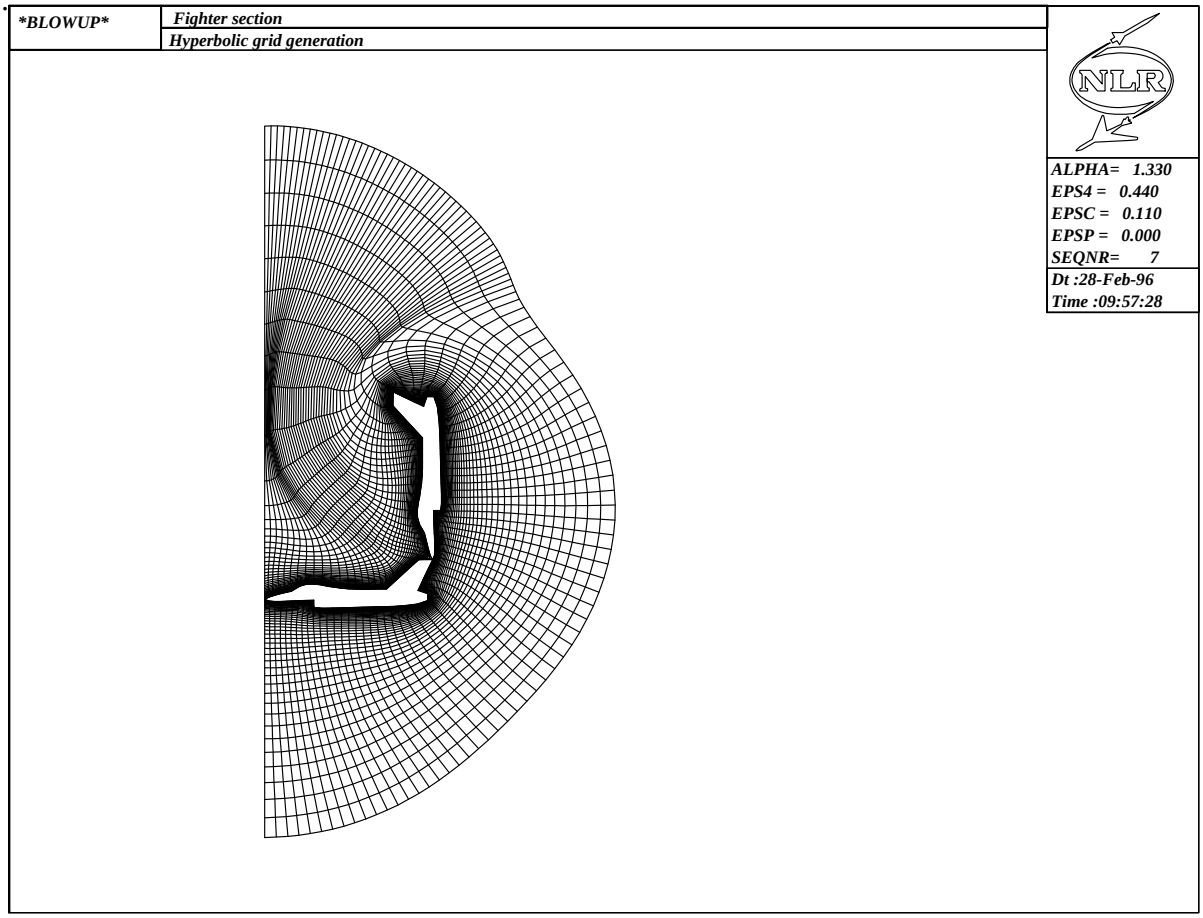

Fig. 3: Mono-block grid generated with a hyperbolic method about a combination of 2 fighters

3.3 Aerodynamic models

The aeroelastic solver is able to carry out the nonlinear aeroelastic analysis in the subsonic and transonic speed range. The extension to the supersonic speed range is easy and has to be made yet.

At present the time-accurate flow is modeled by the unsteady full potential equation, completed by the Clebsch potential model for flows with strong shock waves 3 which takes into account entropy and vorticity corrections.

The choice for this model, mainly motivated by operational requirements with respect to turn-around time and computational costs, is discussed in 4.

Recent enhancements to the model are the inclusion of corrections for viscous effects. A viscous wedge model and a quasi-simultaneous coupling with a boundary layer method have been implemented.

Finally we anticipate the embedding of the solver described in 6, 9 based on the Thin Layer Navier Stokes equations later this year in the AESIM core. The latter extension is motivated by the military drive.

3.4 Simulations

The present version of the method enables the following types of simulation around 2-D and 3-D configurations:

1. Steady aerodynamic simulation at given M_∞ and angle of attack for rigid configuration;
2. Steady aeroelastic simulation with static deformations at given M_∞, angle of attack and dynamic pressure;
3. Unsteady aerodynamic simulation for forced motion, deformation or gust at given M_∞ , angle of attack, vibration mode and type of the motion (gust) (sinusoidal, impulse, jump, polynomial, etc.);
4. Unsteady aeroelastic simulation due to elastomechanical motion or deformation at given M_∞, angle of attack, dynamic pressure and vibration modes. Also an external force due to exciters (flutter vane, gusts) can be included.

Simulations can be performed about symmetric configurations with symmetric and/or anti-symmetric vibration modes with respect to the xy and xz planes. Also simulations are possible for wing-tail configurations and for complete bodies which require circumferential periodicity conditions to be applied.

On slit surfaces emanating from apices or non-trailing edge body parts the imposing of a hard wall, a free jet or a undisturbed pressure condition can be imposed.

3.5 Elastomechanical model

The elastomechanical model is split into a static part and a dynamic part which are explained in the following sections. The static deformation of the aircraft configuration is obtained by means of the 'free-free' flexibility matrix. The dynamic structural behavior of the aircraft is based on the generalized modal deflection approach. The dynamic deformations are expressed in generalized coordinates q_i and their associated modal mass M, damping D, stiffness K and vibration modes $\vec{h}_i$. For a description see 4.

3.6 A(ero)E(lasto) Transfer

The information transfer at the fluid/structure interface is performed by the interpolation models which are well described in 5.

From the implemented interpolation models (see 4) it has turned out in applications that the Least Squares Polynomial approximation of the data and Hounjet's volume spline interpolation method are attractive to select because they do not require any user preparation or intervention. The well-known planar surface spline interpolation and its curvilinear application are hardly used in applications.

In general it is assumed that the elastomechanical data are obtained through NASTRAN so that for this case the interface NASAES has been created.

3.7 Others

Besides the vibration modes, other sets of geometric disturbance fields (control modes, pseudo vibration modes) which are interpolated by the volume spline or polynomial spline method might be specified by the user. These modes are also described in 4.

In order to facilitate the comparison with other reference pressure data during the simulation, the volume spline method is also used to interpolate arbitrary data to the aerodynamic surface grid.

3.8 Time signal analysis

One of the fundamental tasks in an aeroelastic analysis is the determination of the frequency and damping of aeroelastic modes (e.g. to detect if one of the generalized displacements becomes unstable and flutter will occur). As many different time response signals may have to be analyzed several methods for curve-fitting should be available. In general each time response signal exists of contributions of various modal modes, of which the frequency and damping of each one have to be determined.

Therefore, during an unsteady simulation the data must be analyzed on-line in the time domain in order to determine the behavior of a coupled system. The main purpose of this analysis is to determine the frequency and damping characteristics of the discrete time signal. To fulfil that task the following methods have been embedded:

1. The exponential sine fit,
2. Prony's method,
3. Fast Fourier Transform analysis,
4. Curve-fitting of transfer functions.

Since a wide array of time response signals is available several ways exist to make use of the above-mentioned time-fitting tools. The most common time response signals which can be used to determine the frequency and damping characteristics of the discrete time signal consist of:

1. For every modal mode separately:
   - the generalized coordinate,
   - the velocity of the generalized coordinate,
   - the generalized force.
2. Also a combination of modal modes and/or the pressure or deformation data at selected points can be analyzed.

3.9 Monitoring and Postprocessing

Direct monitoring and analysis of all aeroelastic quantities of interest are of major importance to the user. The monitoring of the system is able to provide a graphical presentation of the deformations and pressure distribution on the configuration at selected time samples as well as the mean steady pressure distribution and its first harmonics over a selected time interval. Furthermore, the monitoring is able to provide the dynamic response of integrated loads as lift and moment coefficients for complete configurations as well as individual components. Also the pressure coefficients might be compared with:

1. Pressure coefficients generated at a different time or iteration index which is important for checking convergence.
2. Pressure coefficients generated in a different session which is important for checking different modelings (e.g. full potential against quasi-Euler).
3. Arbitrary reference pressure (experimental) coefficients during the simulation which is important for identification. The volume spline method is used to interpolate the arbitrary data to the aerodynamic surface grid.

When the aeroelastic equations are solved for several flow conditions (variable Mach numbers, angles of attack, amplitudes and frequencies of oscillation) facilities are available to monitor and predict the derivatives of the unsteady airloads in that range and to estimate the critical flutter speed.

Attention has been paid to provide the user with 2-D and 3-D plot and analysis facilities to inspect and analyze all aeroelastic quantities of interest during the simulation. At any time the user may interrupt the program for the analyses and inspection of the data. Again this strongly reduces the workload of the aeroelastician who is not directed to other programs for visualization. The visual output includes screen output and off-plot PostScript output.

Except for the mean and first harmonic components of the aforementioned data which is only available after finishing a complete period of a harmonic motion, the data may be required by the user at any time or iteration step.

3.9.1 Visual Inspection: screen and PostScript plots

Two kinds of visualization tools are available:

- A 2-D facility for plotting collections of 2-D abscissa-ordinate plots gathered on one screen or on multiple screens.
- A 3-D facility for plotting collections of 3-D surfaces with contour plots and/or vector plots on one screen or on multiple screens.

The facilities may be used to plot the aforementioned quantities depending on the type of simulation. The plots can be stored in color PostScript format (using the special options in the interactive plot facility or using screen dump techniques in combination with other plot facilities.

4 AEroelastic SIMulation process

Applying the AEroelastic SIMulation system for the time-accurate simulation of fluid-structure-interaction requires initially:

- an aerodynamic jig-shape geometry,
- a jig-shape elastomechanical model (mode shapes and generalized data) of the structure provided by a FEM package e.g. NASTRAN.

To obtain an aerodynamic jig-shape geometry is rather straightforward, the acquisition of an as accurate as possible elastomechanical model may take months of FEM modeling, hopefully validated by vibration tests. A formidable practical problem, from the start, is consistency between aerodynamic and structural reference values.

The basic operations necessary for a simulation session are in chronological order:

Geometry manipulation on aerodynamic geometry using FOLDIT.

Surface grid generation on aerodynamic geometry using FOLDIT.

Grid generation initiated from the surface grid using BLOWUP.

Interpolation of elastomechanical data on the aerodynamic surface grid.

Steady flowfield calculations on the grid using the steady **solver** for a *chosen Mach number* and *angle of attack*. At the same time the structural deformation under steady aerodynamic loading is calculated.

Simulation consisting of:

1. Specification of the *simulation parameter* (*Mach number* and *angle of attack* remain at their steady values), being *altitude* in case of flight simulation, or *total pressure* in case of wind tunnel simulation.
2. Calculation of successive time steps [1] by alternate solution of the aerodynamic equations in the unsteady **Solver** using boundary conditions through exchange with the elastomechanical equations in the **Motion** module.
3. Monitoring of the flowfield, the elastomechanical model or the amplitude and frequency at any given time using the **Monitoring** module.

[1] The time step should be selected such that the aerodynamics and the elastomechanics remain stable and accurate. Apart for stability and accuracy criteria which stem from the applied solvers it is worthwhile to perform an initial check by running the aerodynamic part of the system and the elastomechanic part separately without coupling at the selected timestep for a number of timesteps

4. Decision on:
   - stop the simulation and end the session after one combination of *Mach number*, *angle of attack* and *altitude*. This results in a time trace of physical parameters comparable to those obtained in real test flights.
   - stop the simulation, go back to item 1, select a new flight *altitude* and start a new simulation. Two or more repetitions of this procedure will enable the operator to create a *flutter diagram* using the **Postprocessing** module.
   - stop the simulation, go back to **steady flowfield** calculation, select a new *Mach number* or *angle of attack* and start a new simulation. Several repetitions of this procedure will enable the operator to create a $C_l - \alpha$-diagram or a *flutter boundary diagram* using the **Postprocessing** module.

   If there is enough information beforehand available these above mentioned procedures can be automated.

In figure 4 is indicated how the time is spent in applying the AESIM system. Also included in this figure is an estimate of manpower and computer power required in time. The scales represent a maximum of 100 percent. The dotted lines represent required power and the solid lines represent available power. As can be seen from this figure, generating a grid (BLOWUP), interpolating the mode shapes onto the grid and obtaining a steady flow field may take a day each, whereas obtaining a surface grid using FOLDIT may take weeks. The initial phases in the operational strategy might take a week and the simulation even longer. When it comes to CPU power, to the right of the figure, there is a severe limitation when the cycle reaches the simulation stage and turn-around-time is severely bounded by the available CPU power. When it comes to manpower, to the left of the figure, the maximum effort is required at the beginning of a new case in the geometry manipulation part of the module FOLDIT. This is a result of the fact that every new geometry may contain difficulties not yet encountered during earlier cases. From the beginning the effort reduces as a result of going through a learning curve. Solutions to the aforementioned difficulties were fed back into the FOLDIT computer code, which has been improved considerably and will be so probably in the future. Also at the start of a new simulation considerable effort is needed to obtain a proper nondimensionalization of all physical quantities involved and to guarantee that simulations are performed to the part of the flight envelope which is prone to instabilities. The required manpower will not become zero during the cycle, because the simulation has to be monitored, although it reaches a minimum during this process.

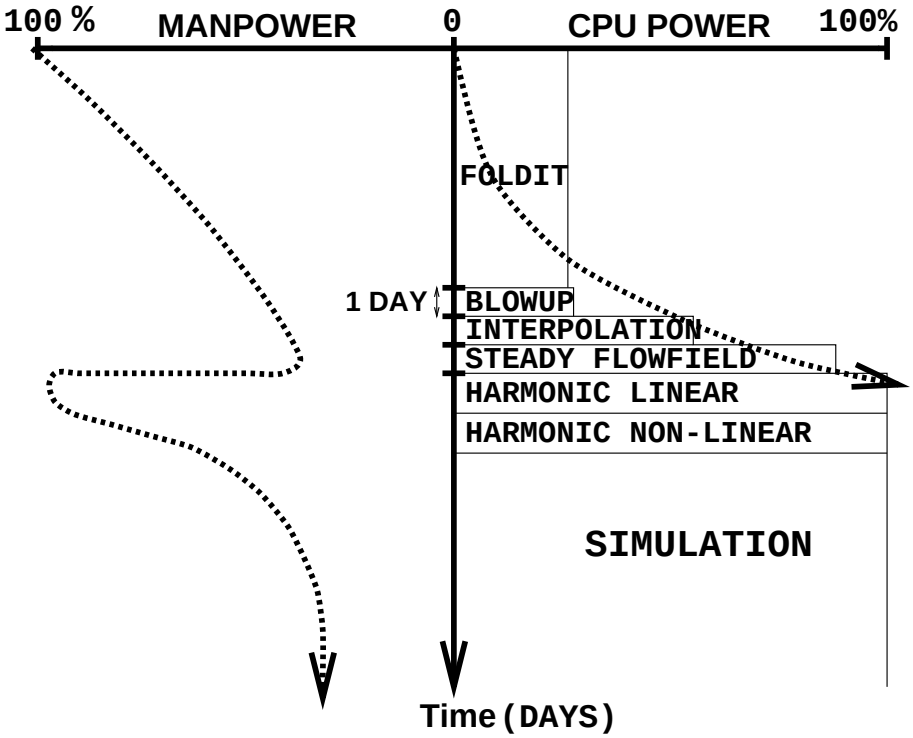

Fig. 4: CPU power and manpower versus time for the AEroelastic SIMulation system

To prohibit an unduly long repetition of the simulation cycle an operational strategy is essential.

4.1 Operational strategy

Experience with AESIM has shown that the best way to tackle an aeroelastic problem - not investigated or documented by anyone before - is to pass three stages:

1. Use a combination of K or PK-method and linear (e.g. Doublet Lattice (GUL)) aero. This will give a quick global view of the dynamic entities of the problem at issue, for instance the number of mode shapes involved, and a starting value of the reduced frequency range in which flutter can be expected. An example is shown in figure 10. The reduced frequency range obtained this way will be used in the next stage. Also in this stage it is relatively easy to obtain consistency between the geometrical and elastomechanical data sets.
2. Apply the PK-method with harmonic generalized forces, calculated by AESIM for forced harmonic motion (or pulse response or with the diverging rate approach, once available) of the different mode shapes. From this a more accurate impression of the dynamic characteristics is obtained.
3. This flutter diagram will act as a guideline to trace troublesome operational areas and give starting values for the nonlinear direct simulation of the aero-structure coupling in AESIM to

gain detailed insight in the damping, frequency and amplitude behavior of the structure. To obtain the flutter boundaries in the direct simulation, time response signals of the generalized coordinates are needed, which contain at least 3 cycles of the longest wavelength in the problem. Since the ratio of relevant short and long wavelengths that must be considered is usually about 10, approximately 30 cycles of the highest frequency component need to be modeled. Since the accurate modeling of one cycle takes about 256 AF sweeps (128 time steps with 2 subiterates) one needs about 7500 AF sweeps to obtain the damping characteristics for one condition. For lowly damped systems the situation might be much worse.

A typical example is shown in figure 11.

5 Applications

The applicability range of the method is directed to 2-D airfoils, 3-D wings, 3-D wing-bodies, T-tails, etc. In this paper some applications of the method will be presented, which were not shown already in 3 and 4 and involved applications with and without the Clebsch potential to 2-D airfoils and 3-D wings and T-tails. The examples here will focus on current ongoing activities in 3-D and demonstrate the status of the aeroelastic environment.

Running the examples produced invaluable experience, which was fed back into the computer code of the different modules and is discussed below.

5.1 Experience and Feedback

- **Geometry manipulation**
  - **Experience** In all examples shown here the geometry was obtained in the form of a number of so-called parent segments containing discrete data.
    The major problem is to subdivide and modify the parent segments such that a set of unique child segments results, each uniquely connected to neighboring child segments by their vertices.
    In the ideal situation which hardly ever occurs in practice, the parent segments already satisfy the aforementioned property and the manipulation stage can be skipped.
    This was certainly not the case for the T-tail fuselage , as the ICEM-CFD segments contained properties, such as apices and random normal directions, not initially foreseen in FOLDIT.
    For the fighter, starting from the complete geometry coming out of ICEM-CFD, see figure 13, once again considerable effort was needed to produce a surface grid, due to the need to modify the geometry.
    The ultimate test for the geometry manipulator, FOLDIT, constitutes the fighter configuration with a slender store installed at the wing tip. The tip store geometry separately could be manipulated by FOLDIT but the consequent mating to the wing tip of the already modified fighter turned out to be very time-consuming due to the difference in length scale of the store and the fighter geometry.
    The color wireframe graphics applied in the method are felt as a limitation. The public domain package GeomView was tested, however it could not succeed requirements in sufficiently fast visualizing a 3-D surface on a medium sized workstation.
  - **Feedback** As turn-around times made it impractical to try to fix the experienced problems by returning to the CAD/CAM or ICEM-CFD software, the choice was made

to incorporate the experience gained into the FOLDIT computer code by equipping it with segment merging and redistribution tools and a normal direction finder with equalizer. Also tools emanating from the need to modify the geometry were developed, such as the construction of new elements.

Although the subdivision and connection process is completely automated, offsets in the geometrical definition may cause failures and require the users' intervention and interference (subdivision or modification).

The process has been fully automated through use of scripts, command and PostScript logging files, which give the user flexibility and the possibility of exact reproduction and provide debugging material for the code developer.

- **Surface grid generation**
  - **Experience** Initially the distribution of the surface grid had to be adjusted by hand for every individual segment. For practical examples this proved to be a nuisance.
  - **Feedback** To ease the generation of a surface grid the **domino** approach was introduced. This process has been fully automated through use of scripts.
- **Field grid generation**
  - **Experience** Ordinary modeling and software problems were encountered.
  - **Feedback** This process has been fully automated through use of scripts.
- **Interpolation**
  - **Experience** From experience the least squares and the volume spline routines come up to expectation.
  - **Feedback** None.
- **Solver**
  - **Experience** Every new application has flow areas not investigated before, that might effect stability due to inadequate modeling and/or software problems.
  - **Feedback** Monitoring is indispensable in tracing these areas. Without monitoring the debugging of the complex solver would result in a serious handicap for the code developer.
- **Time analysis**
  - **Experience** There is no standard strategy for fitting time traces in order to obtain frequency and damping data of the dynamic system. Using MATLAB was not successful.
  - **Feedback** Several combinations of fitting methods are used. Previously obtained data is used as starting values for the fitting procedures.
- **Operational Strategy**

– **Experience** In every new application it was not easy to obtain consistency between the geometrical and elastomechanical data sets. This is due to the many disciplines which are involved, each favoring its own nondimensionalizations and coordinate systems. moreover, new applications need indications where the zones of flight instability might be located. This will reduce the required computational resources.
– **Feedback** The first two stages in the operational strategy are introduced for the aforementioned consistency and localization reasons.

5.2 T-tail

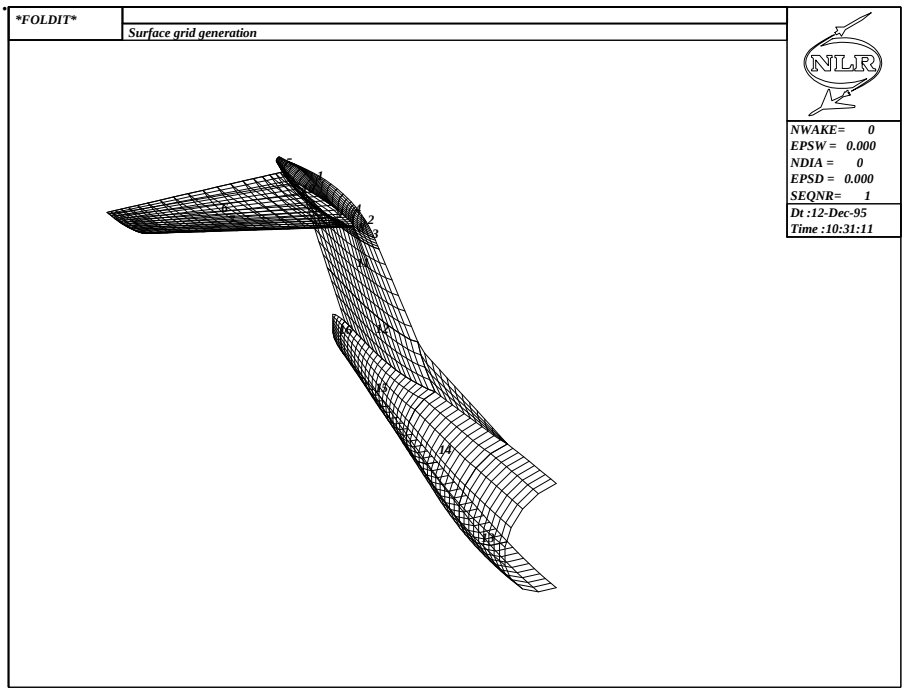

Fig. 5: T-tail geometry input for FOLDIT

In order to demonstrate the ability of the system to deal with existing aircraft structures a transport-type T-tail fuselage configuration was considered, see figure 5. It should be noted that no parts of the geometry were omitted. The complete geometry from ICEM-CFD was processed by FOLDIT, in order to obtain a surface grid. The surface grid initiates the volume grid of which characteristic grid planes are depicted in figure 6 and show the ability of the grid generator to deal with strongly swept wings and non-uniform distributions. For the grid 67x30x33 nodes were applied. Figure 7 shows the steady pressure distribution on the horizontal tail. From top left to bottom right pressure distributions at different spanwise stations from root to tip are depicted. A considerable transonic effect is apparent. Figures 8-9 show the first and second mode shapes of the T-tail configuration.

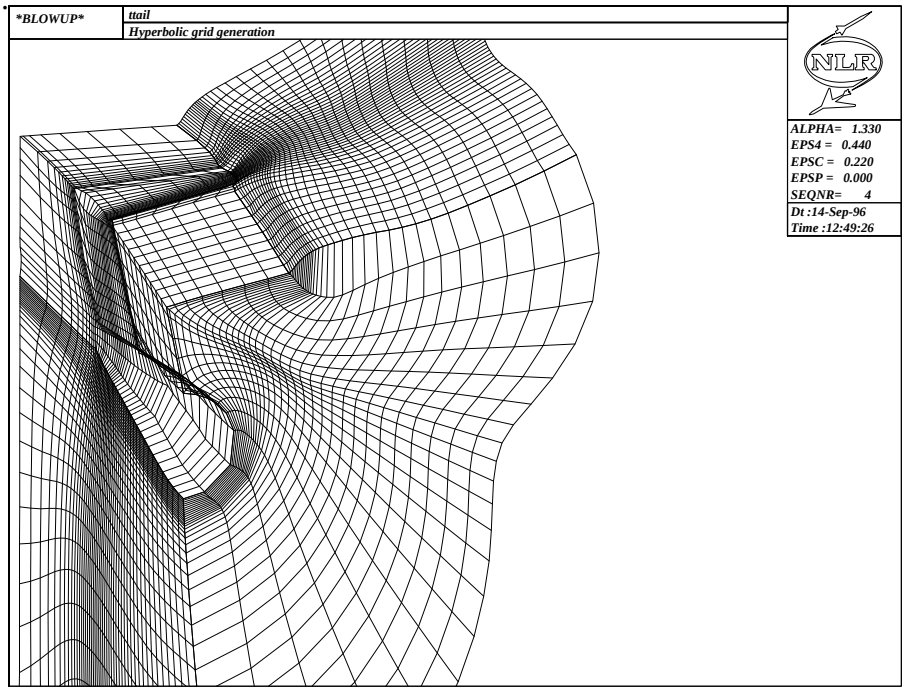

Fig. 6: Characteristic grid planes of the T-tail

The flutter diagram, obtained using the PK-method, in figure 10 shows a strong coupling between the first and second mode shape. Unsteady calculations were performed at $M_\infty = 0.84$ and zero altitude in Standard Atmosphere. The elastomechanical model consisted of ten modes. The generalized coordinates of each individual mode were calculated in time as a result of a non-zero initial value for the acceleration of the generalized coordinate. In figure 12 the time response information is evaluated through signal processing to get damping and frequency information. The results of these simulations confirm that the T-tail has a stable dynamic behavior for the flight condition under consideration. This is in accordance with the MSC/NASTRAN flutter diagram.

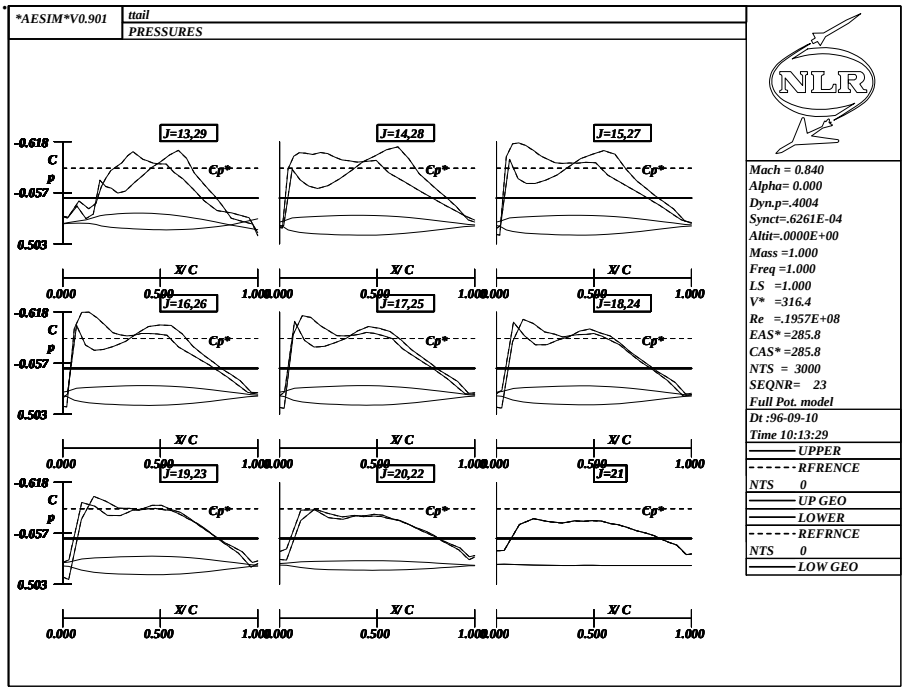

Fig. 7: Steady pressure distribution on horizontal tail

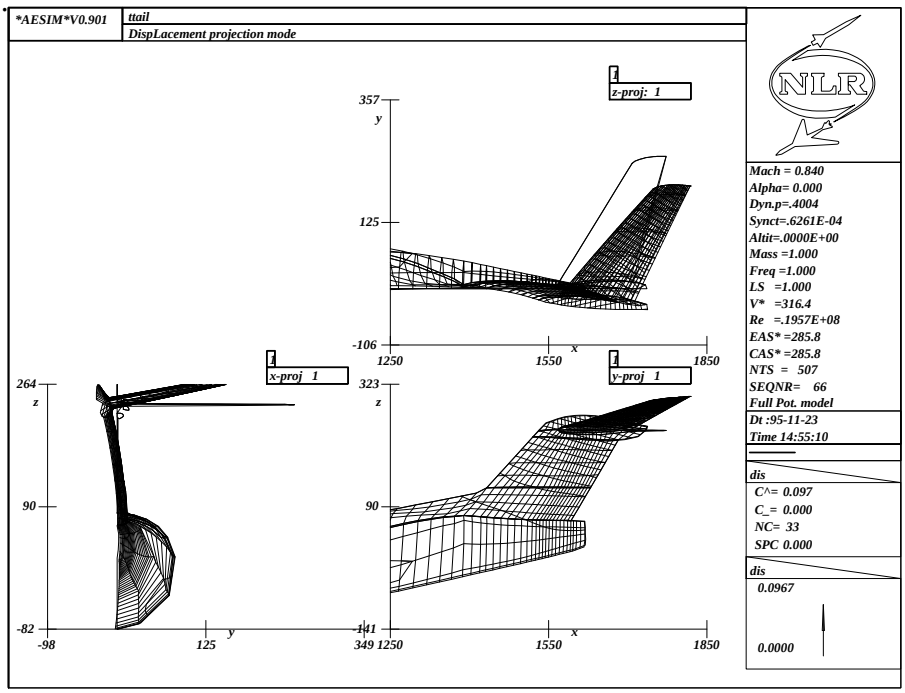

Fig. 8: First mode shape of T-tail

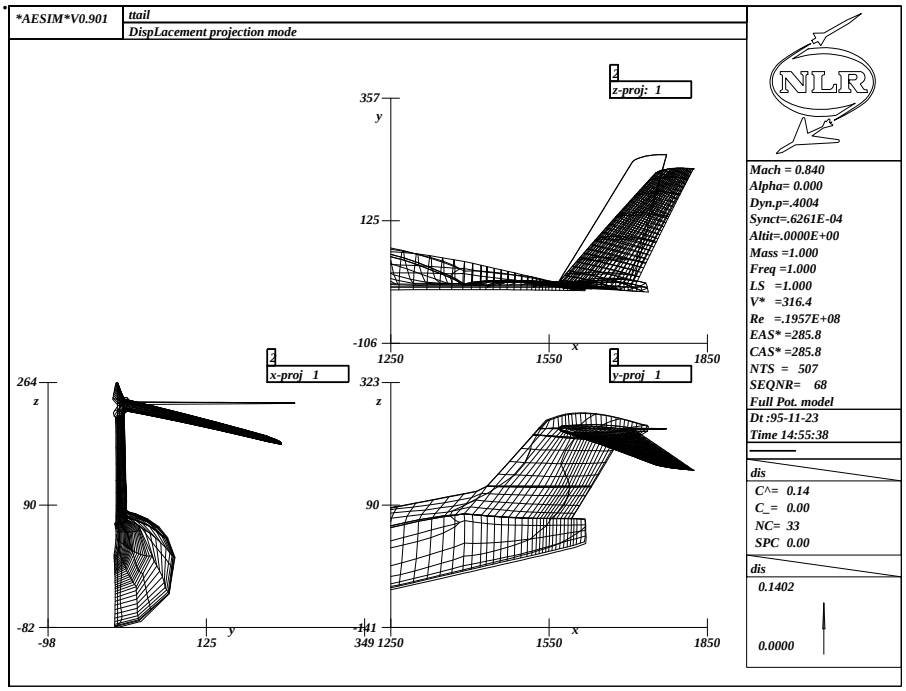

Fig. 9: Second mode shape of T-tail

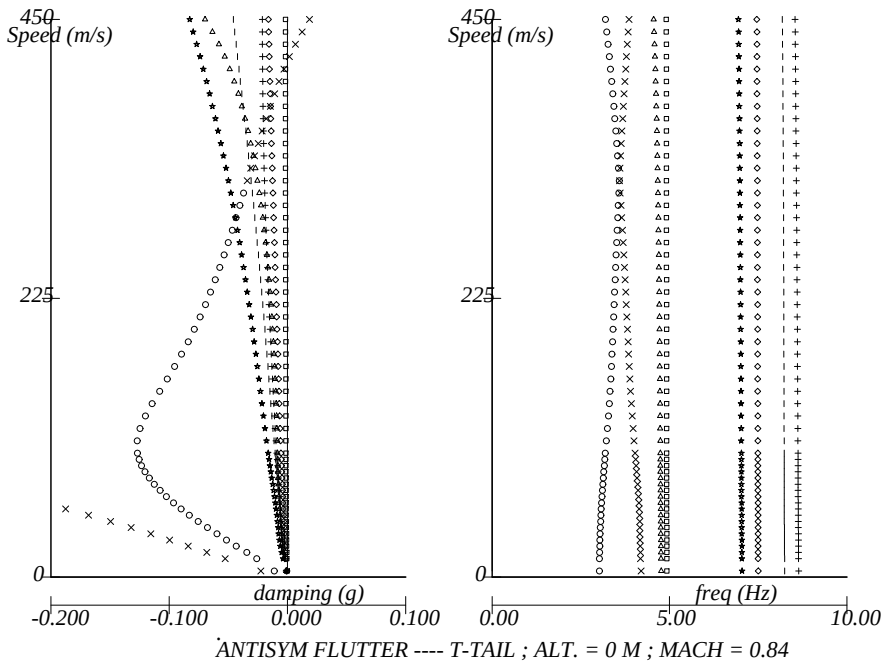

Fig. 10: Flutter diagram of T-tail using PK-method with MSC/NASTRAN

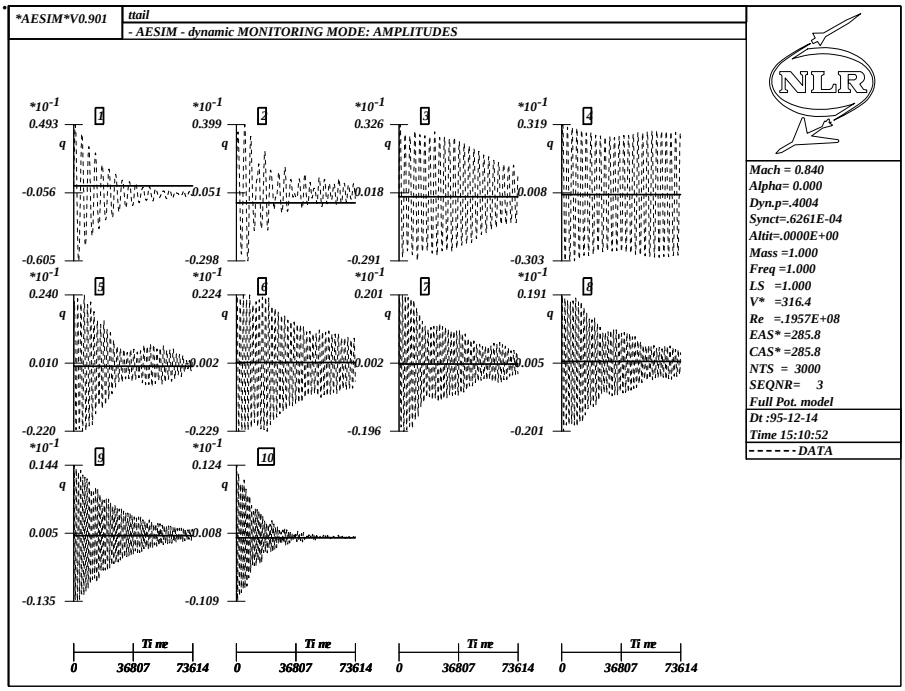

Fig. 11: Ten modes dynamic response of generalized coordinates at Mach=0.84 and zero altitude in Standard Atmosphere

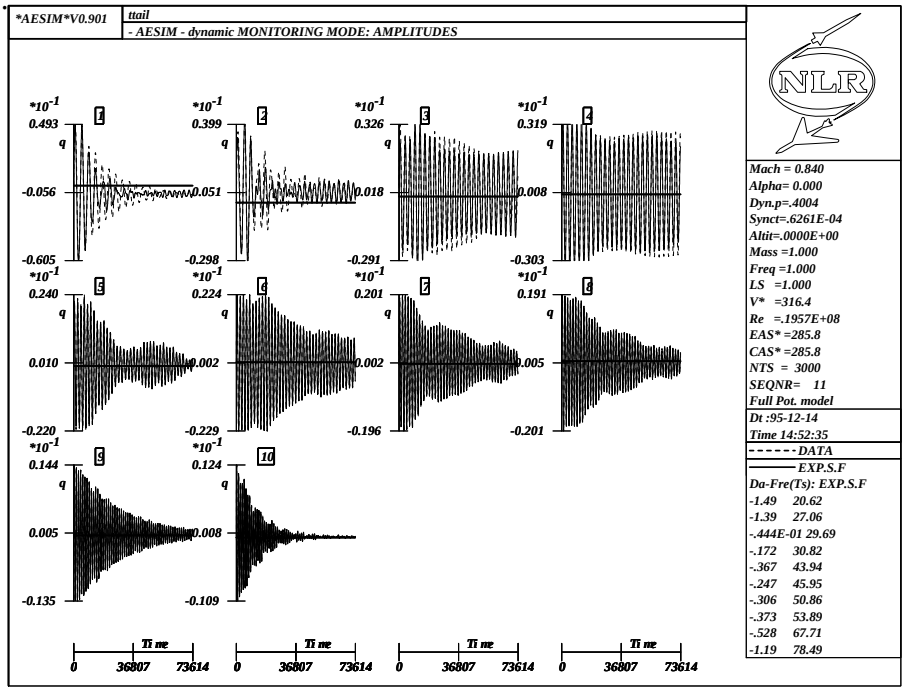

Fig. 12: Result after signal processing of dynamic response of generalized coordinates at Mach=0.84 and zero altitude in Standard Atmosphere

5.3 Fighter configuration I

In view of the future development of aerodynamic solvers the ability of the aeroelastic simulation system to deal with fighter-type configurations has been considered. The fighter configuration has been altered to resemble a wind tunnel model, of which steady and unsteady pressure data are available, 7. Figures 14-15 show the alterations to the forebody. Here the concavity of the diverter over the engine air intake and the intake itself had to be closed. Figures 16-17 show the alterations to the aft body. Here the vertical, horizontal and ventral fins had to be removed.

Once the surface grid was ready the volume grid was generated by pressing a button. Figure 19 shows characteristic grid planes of the fighter geometry. For the grid 72x34x27 nodes were applied. The steady flowfield calculation generated isobars as shown in figures 20 and 21. Here a comparison is made of pressures on the upper side between calculations and volume-splined experimental results. Notwithstanding the limited validity of the full potential equations, the comparison looks surprisingly good. Note that the condition of Mach=0.92 and α=6 deg is on the border of applicability of the flow solver.

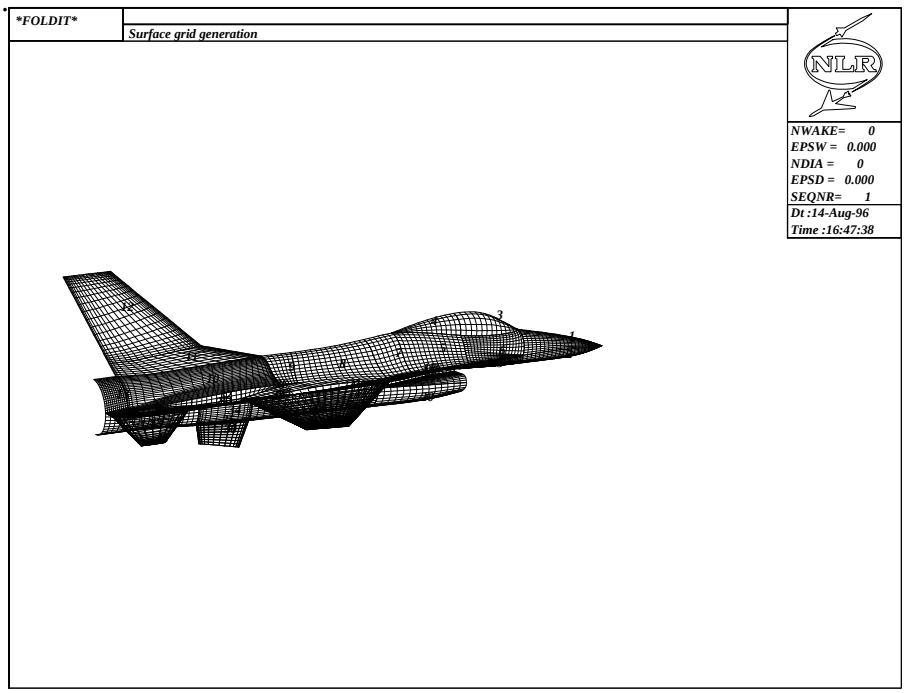

Fig. 13: Fighter geometry input for FOLDIT

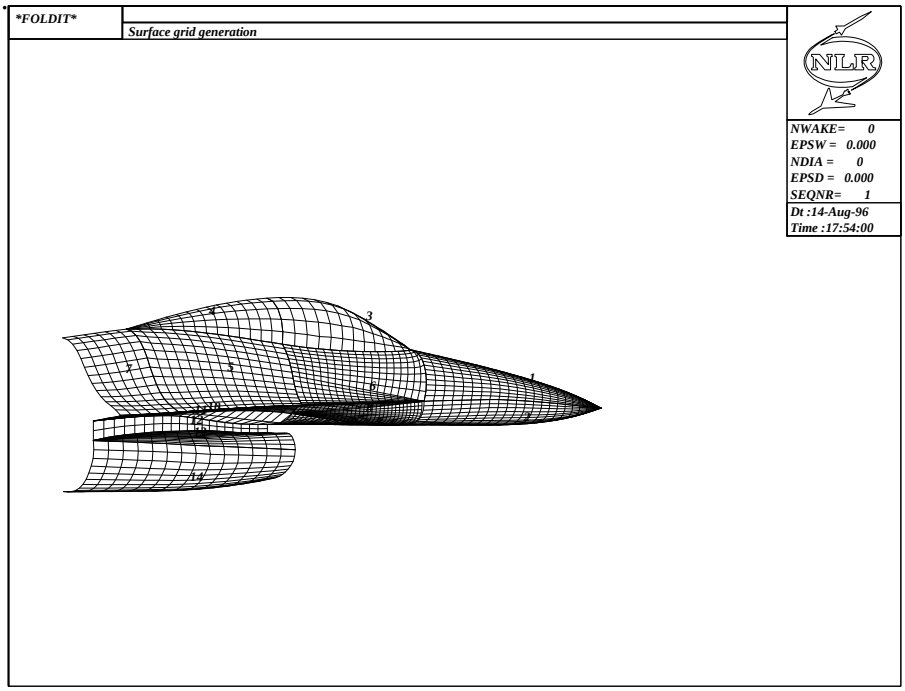

Fig. 14: Original fighter forebody geometry

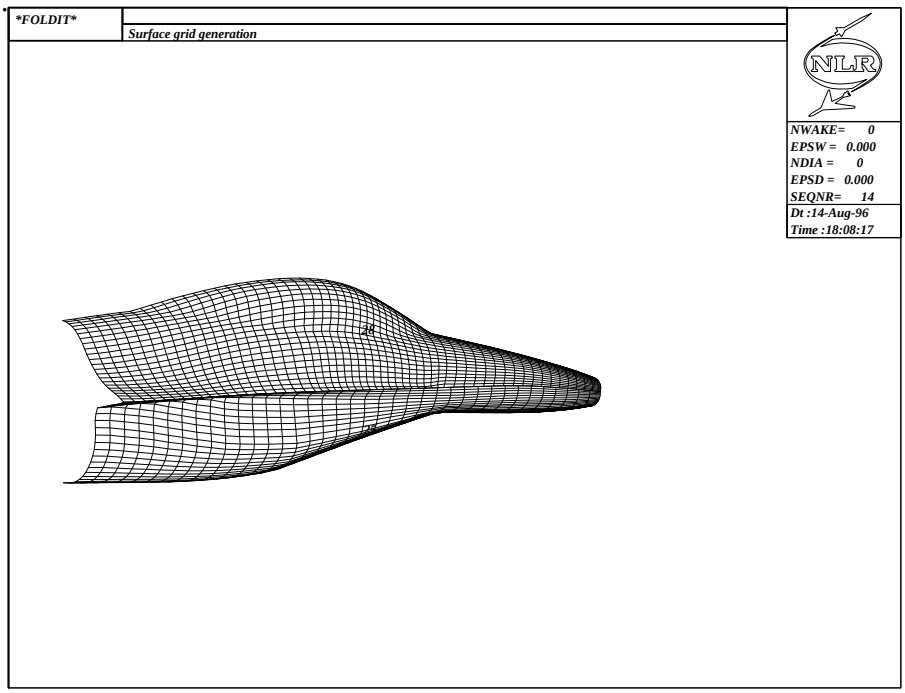

Fig. 15: Closing of the diverter over the engine air intake, clipping of the nose cone and closing of the engine air intake

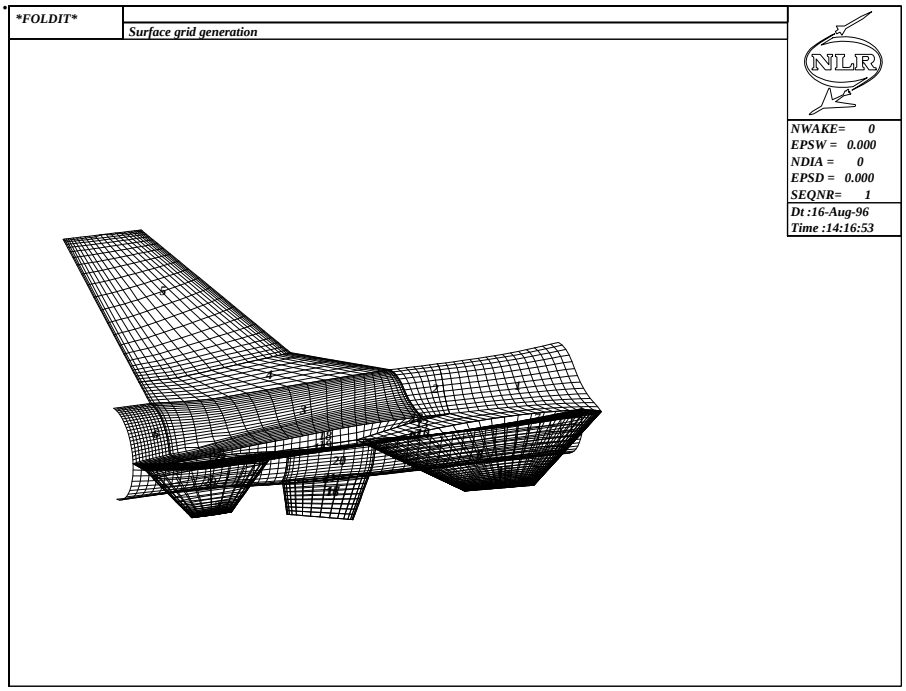

Fig. 16: Original fighter aft body geometry

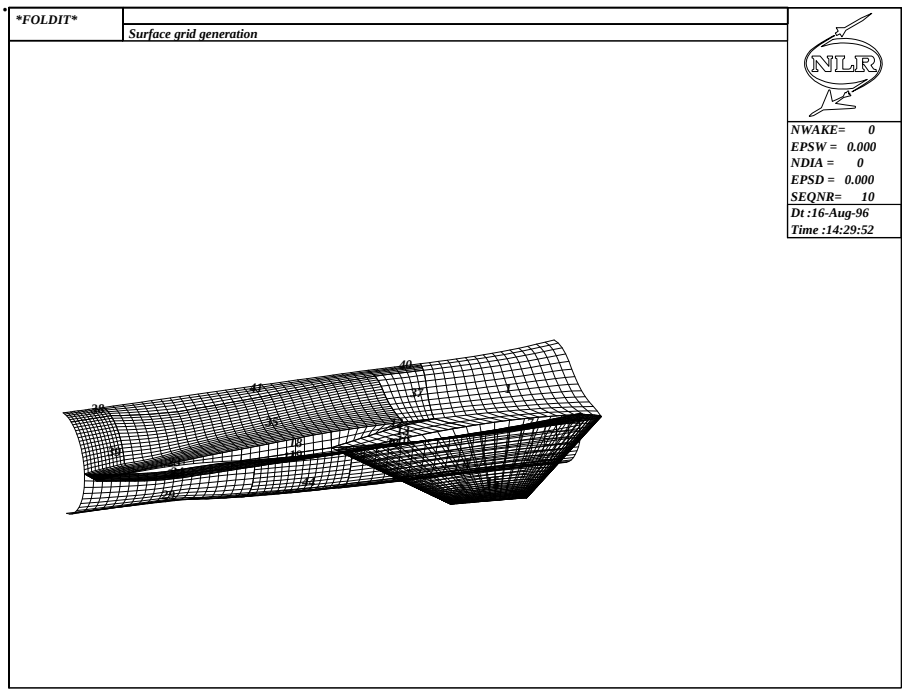

Fig. 17: Modified fighter aft body geometry

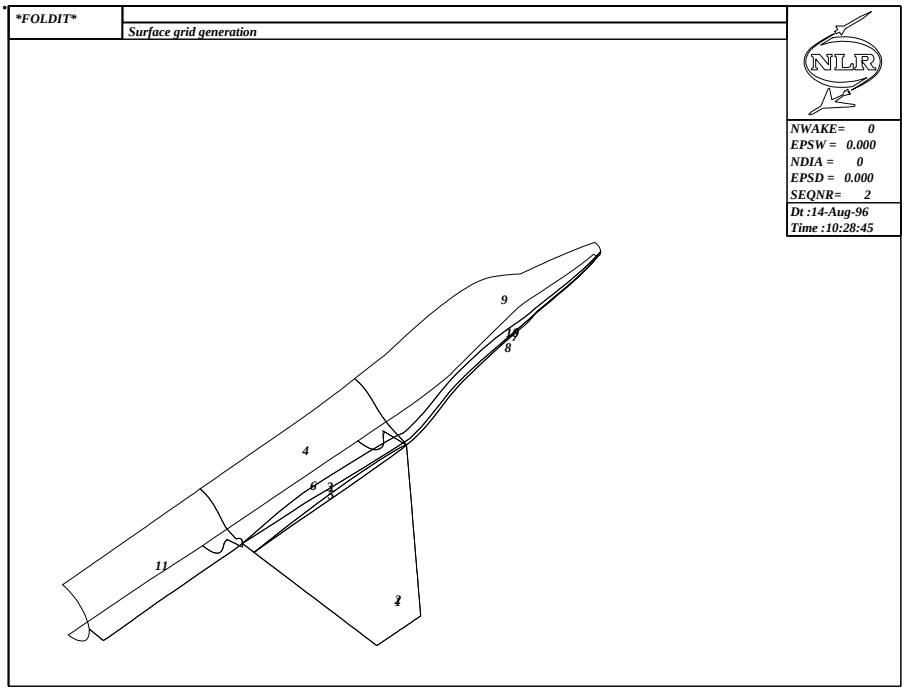

Fig. 18: Segment edges of modified geometry

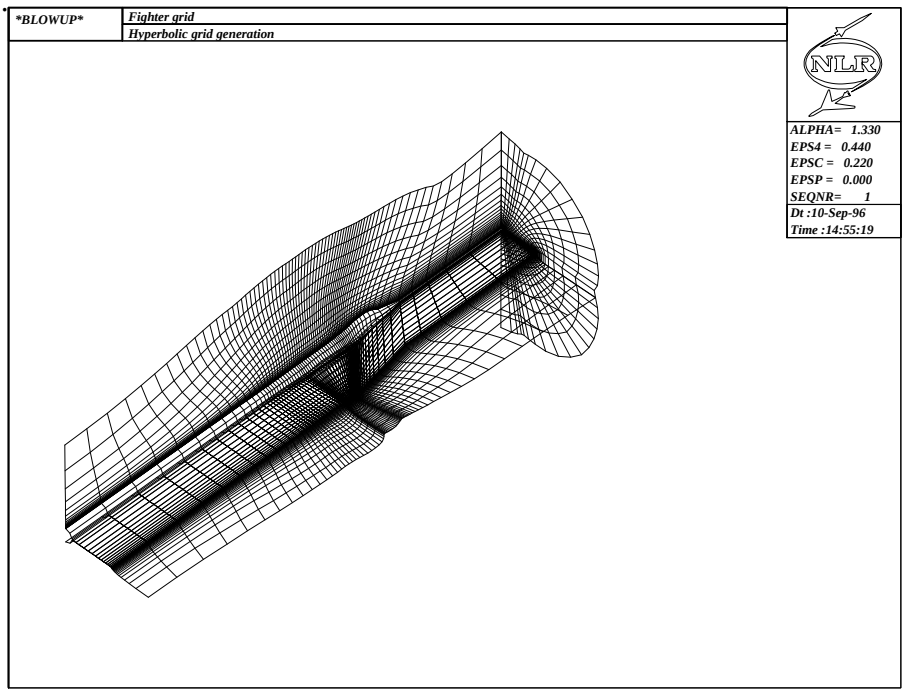

Fig. 19: Characteristic gridplanes of fighter

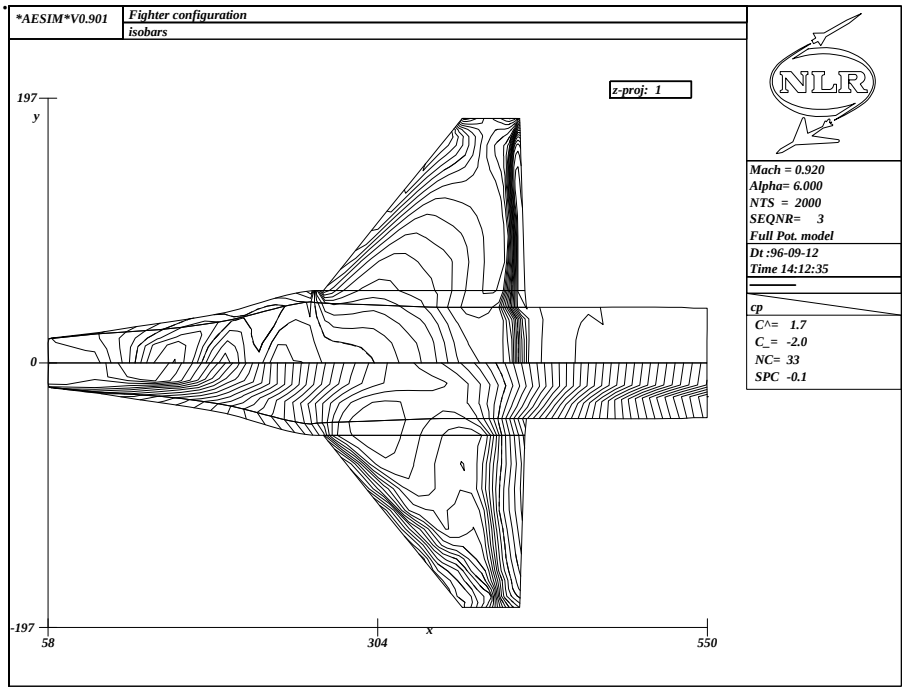

Fig. 20: Isobaric footprint of upper side of fighter, containing volume splined experimental data on the negative y-axis, for Mach=0.92 and α=6 deg

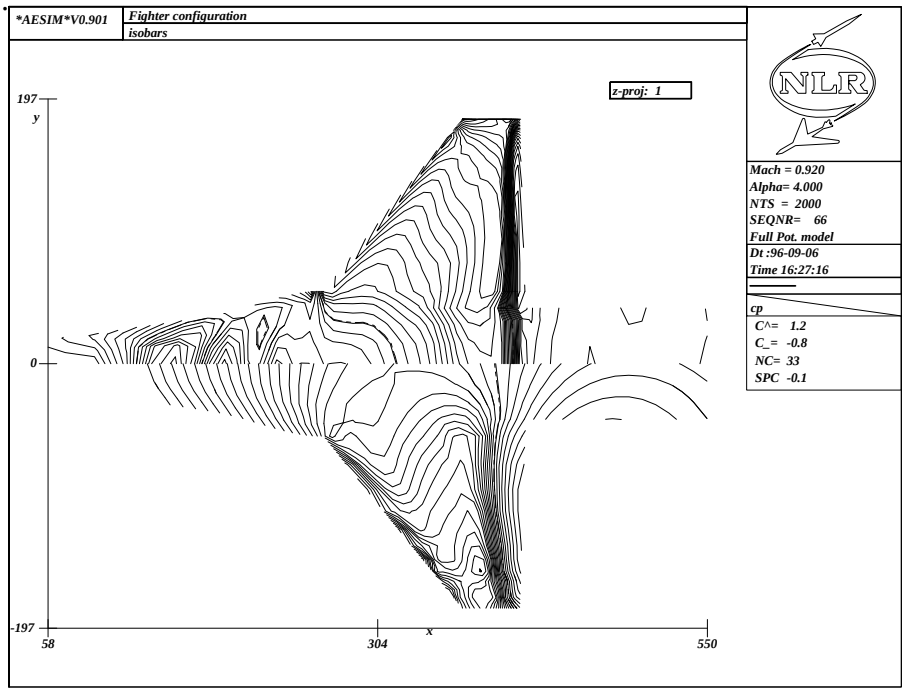

Fig. 21: Isobaric footprint of upper side of fighter, containing volume-splined experimental data on the negative y-axis, for Mach=0.92 and α=4 deg

5.4 Fighter configuration II

The geometry of the fighter with tip store is shown in figure 22. The surface grid obtained by FOLDIT is depicted in figure 23 and the surface grid with far wake slits and far diaphragms in figure 24. The volume grid was generated completely automatically. A characteristic cross-section of the grid is shown in figure 25. The proportion between the fuselage and the tip store cross-sectional area is striking in this figure. For the grid 87x46x27 nodes were applied. The result of a steady flow field calculation is shown in figure 26.

Unsteady simulations with fighter configuration I and II are envisaged.

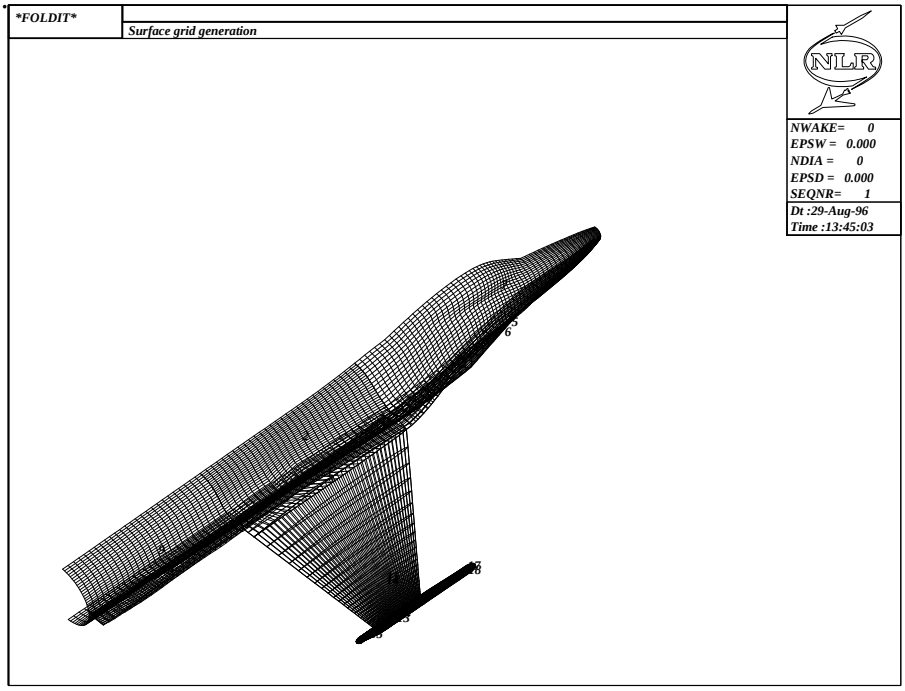

Fig. 22: Modified fighter geometry with slender tip store

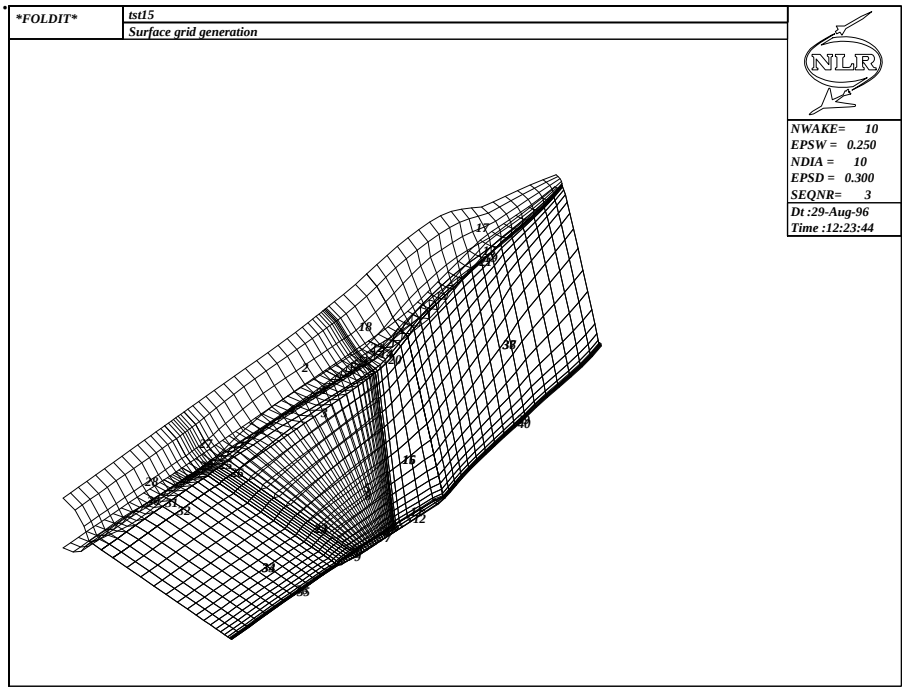

Fig. 23: Surface grid of fighter with tip store provided with diaphragms and wake slits

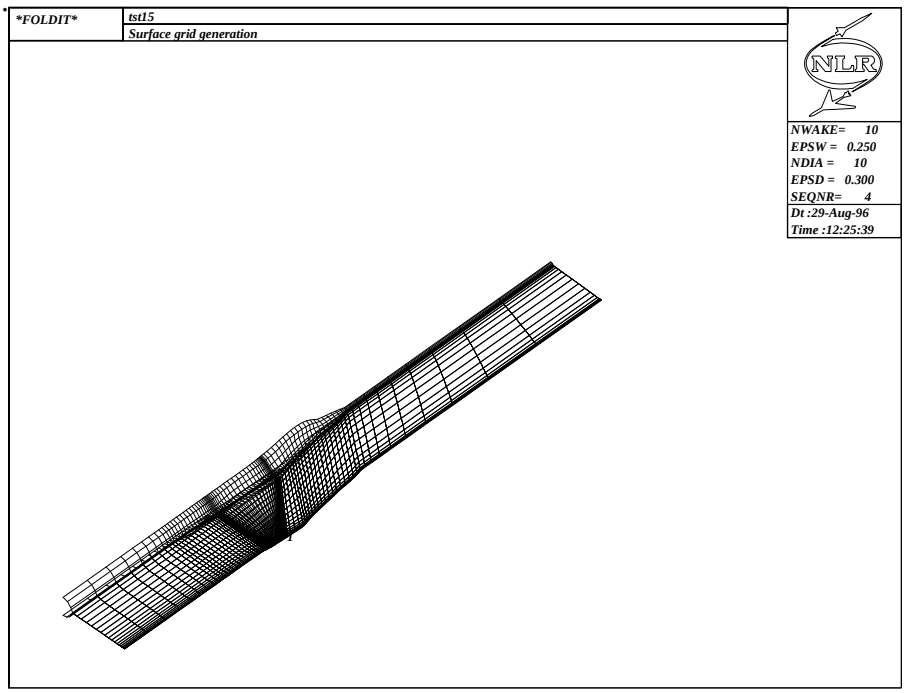

Fig. 24: Surface grid of fighter with tip store provided with far diaphragms and far wake slits

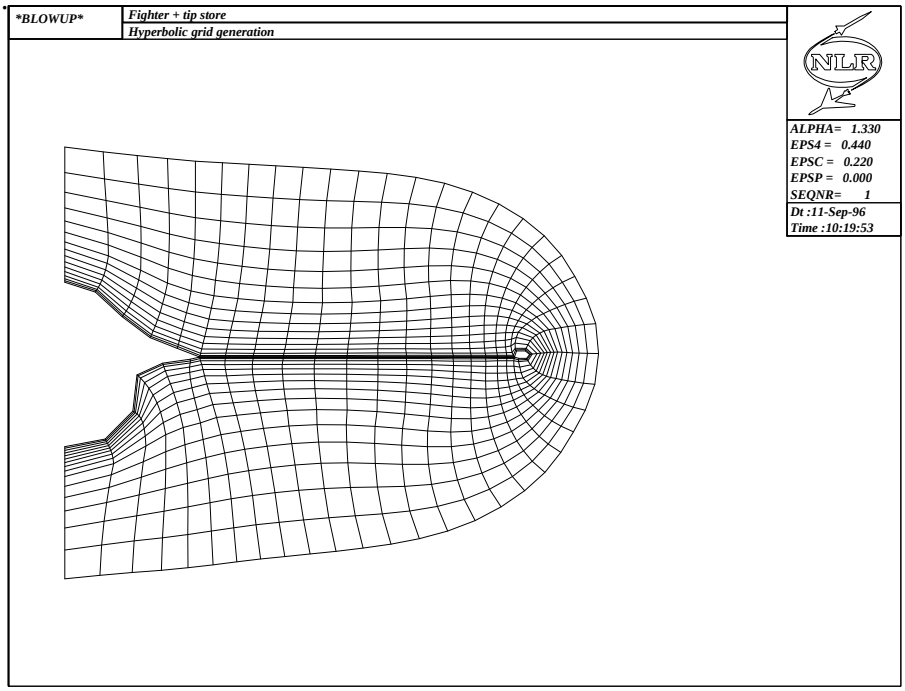

Fig. 25: Grid cross-section just in front of wing leading edge

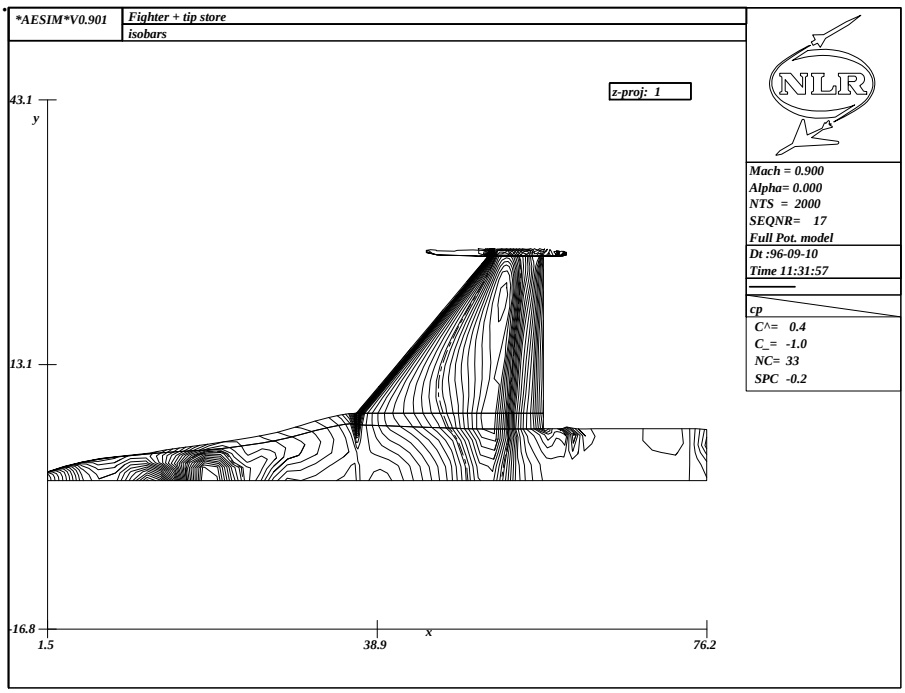

Fig. 26: Isobaric footprint of upper side of fighter with tip store for Mach=0.90 and α=0 deg

6 Conclusion

In this paper the status of the NLR system for aeroelastic simulation has been presented and demonstrated.

Experience with recent applications to complex configurations has led to the following observations:

- The most critical part of the AEroelastic SIMulation system is the geometry manipulation in the surface grid generation module FOLDIT.
- The embedding of the **domino** approach in the surface grid generation module FOLDIT has proven its value.
- The grid generator module BLOWUP has been demonstrated for complex geometries.
- The interpolation at the fluid/structure interface can be carried out satisfactorily with the available models.
- The full potential solver has been applied successfully at the edge of its operational border.
- The volume spline method has proven its value in interpolating experimental data.
- The analysis of timesignals can be carried out satisfactorily with the available models.
- The availability of direct graphical monitoring of all relevant data was crucial in reducing the required CPU time, the required manpower and the development and maintenance of the software.
- The effort to obtain consistency between the geometrical and elastomechanical input data sets is often overlooked in interdisciplinary use.

7 References

1. M. H. L. Hounjet, *Hyperbolic grid generation control by panel methods*, NLR TP 91061 U, June 1991.
2. W.M. Chan and J.L. Steger .*A generalised scheme for three-dimensional hyperbolic grid generation*, AIAA-91-1588-CP, July 1991.
3. J. Westland and M.H.L. Hounjet, *Clebsch variable model for unsteady, inviscid, transonic flow with strong shock waves*, AIAA 93-3025, July 1993
4. M.H.L. Hounjet and B.J.G. Eussen, *Outline and Application of the NLR Aeroelastic Simulation Method*, ICAS-94-5.8.2, September 1994
5. M.H.L. Hounjet and J.J. Meijer ,*Evaluation of Elastomechanical and Aerodynamic Data Transfer Methods for Non-planar Configurations in Computational Aeroelastic Analysis* Contribution to CEAS Symposium: 'International Forum on Aeroelasticity and Structural Dynamics 1995'
6. B. Prananta, M.H.L. Hounjet and R.J. Zwaan, *A Thin Layer Navier-Stokes Solver and its Application for Aeroelastic Analysis of an Airfoil in Transonic Flow* Contribution to CEAS Symposium: 'International Forum on Aeroelasticity and Structural Dynamics 1995'
7. A.M. Cunningham Jr,(Lockheed Fort Worth Company), *Personal Communications*.
8. M.H.L. Hounjet and B.J.G. Eussen, *AESIM: An Aeroelastic simulation method for transport aircraft in transonic flow*, NLR CR 96009 C, January 1996
9. B.B. Prananta and M.H.L. Hounjet, *Aeroelastic Simulation with Advanced CFD Methods in 2D and 3D Transonic Flow*, In Proceedings Conference on Unsteady Aerodynamics, RAeS, London, July 17-18 1996